Liquid Crystals
Publication details, including instructions for authors and subscription information:
http://www.informaworld.com/smpp/title~content=t713926090

Threshold flexoelectric deformations in homeotropic nematic layers

Mariola Felczak[a]; Grzegorz Derfel[a]
[a] Institute of Physics, Technical University of Łódź, ul. Wólczańska 219, 93-005 Łódź, Poland,

Online publication date: 11 November 2010

To cite this Article Felczak, Mariola and Derfel, Grzegorz(2003) 'Threshold flexoelectric deformations in homeotropic nematic layers', Liquid Crystals, 30: 6, 739 — 746
To link to this Article: DOI: 10.1080/0267829031000115014
URL: http://dx.doi.org/10.1080/0267829031000115014

Liquid Crystals, 2003, Vol. 30, No. 6, 739–746

Threshold flexoelectric deformations in homeotropic nematic layers

MARIOLA FELCZAK* and GRZEGORZ DERFEL
Institute of Physics, Technical University of Łódź, ul. Wólczańska 219, 93-005 Łódź, Poland

(*Received 21 November 2002; accepted 23 February 2003*)

Elastic deformations of nematic liquid crystal layers subjected to a d.c. electric field were studied numerically. The flexoelectric properties of the nematic material and the presence of ionic space charge were taken into account. Homeotropic alignment with finite surface anchoring strength was assumed. The director orientation and the electric potential distribution were calculated; the space charge density was also determined. It was found that the threshold voltage strongly depended on the parameters of the system. In particular, a threshold as low as a few tenths of a volt occurred under suitable circumstances. In the case of a negative dielectric anisotropy, $\Delta\varepsilon$, such low values of the threshold voltage existed when the ion concentration was sufficiently high, and given sufficiently large magnitudes of the flexoelectric coefficients and a sufficiently small anchoring energy. If the ion concentration was low or if the flexoelectric coefficients were small or if the surface anchoring was strong, the threshold was equal to several volts. In the case of positive dielectric anisotropy, the threshold amounted to several tenths of a volt for a weakly anisotropic and highly conductive material. If the dielectric anisotropy was sufficiently high or if the ion concentration was sufficiently low, the threshold voltage increased with $\Delta\varepsilon$ and reached tens of volts. These results can be explained as the effect of the inhomogeneous electric field arising in the vicinity of the surfaces, due to the ionic space charge redistributed by the external voltage. They are qualitatively consistent with earlier experiments which show the effect of the ion concentration on the elastic deformations in flexoelectric nematics. They correspond also with theoretical results concerning the effect of the electric field produced by the surface polarization or by the adsorption of ions.

1. Introduction

Electric field-induced deformations of the director distribution in nematic liquid crystal layers are twofold in nature: dielectric and flexoelectric. In general, torques due to both mechanisms may arise in a sample. Nevertheless, the circumstances in which the flexoelectric torques can be neglected are the most common. The torques resulting from the dielectric anisotropy $\Delta\varepsilon$ of the liquid crystal are usually considered as the sole cause of the deformations. They depend on the square of the electric field strength E^2, so the sense of the electric field strength vector $\mathbf{E}$ is of no importance. One can distinguish several simple geometries which have practical significance both for applications and laboratory studies. The deformations occur under strong as well as under weak anchoring conditions [1]. In both cases they have threshold character, at least when a suitable surface alignment is ensured. This means that the external voltage must exceed a certain critical value. For example, if $\Delta\varepsilon<0$, a rigidly anchored homeotropic nematic layer of thickness d confined between parallel electrode plates becomes distorted, provided that the voltage is higher than U_c given by the formula

$$U_c=\pi\left(\frac{k_{33}}{\varepsilon_0|\Delta\varepsilon|}\right)^{\frac{1}{2}} \tag{1}$$

where k_{33} is the bend elastic constant and ε_0 is the permittivity of vacuum. In the case of a finite anchoring energy, the corresponding threshold U_c' is smaller than U_c and is given by the equation

$$\cot\left[\frac{U_c'}{2}\left(\frac{\varepsilon_0|\Delta\varepsilon|}{k_{33}}\right)^{\frac{1}{2}}\right]=\frac{U_c'}{Wd}\left(k_{33}\varepsilon_0|\Delta\varepsilon|\right)^{\frac{1}{2}} \tag{2}$$

where W is the Rapini–Papoular anchoring strength parameter [2]. On the other hand, a nematic with $\Delta\varepsilon>0$ remains undeformed due to the stabilizing influence of the dielectric torque in this case.

*Author for correspondence;
e-mail: mfelczak@ck-sg.p.lodz.pl

Liquid Crystals ISSN 0267-8292 print/ISSN 1366-5855 online
http://www.tandf.co.uk/journals
DOI: 10.1080/0267829031000115014

The other contribution to the deformations induced by the electric field is due to the flexoelectric properties of the nematic material [3]. There are two possible origins of these properties [4, 5], which result in macroscopic flexoelectric coefficients e_{11} and e_{33}. The flexoelectric deformations are due to the torque which is linear with respect to the electric field $\mathbf{E}$ or to the torque resulting from the spatial variation of the field $\nabla\mathbf{E}$. They are difficult to observe since they require rather weak anchoring conditions; they can be masked by the dielectric deformations and be disturbed by the ionic space charge always present in liquid crystals.

The electric field-induced deformations in insulating nematics were comprehensively analysed on the basis of continuum theory. The simple geometry, in which the director orientation is restricted to the plane perpendicular to the layer, is of special interest. In this geometry, sixteen configurations of the liquid crystal layers subjected to an electric field were distinguished [6]. In eight of these configurations, the deformations have threshold character. In particular, the homeotropic layer with symmetrical boundary conditions containing the $\Delta\varepsilon<0$ nematic becomes distorted above the threshold U_f given by the equation

$$\cot\left(\pi\frac{U_\mathrm{f}}{U_\mathrm{c}}\right)=\frac{Wd}{2\pi k_{33}}\frac{U_\mathrm{c}}{U_\mathrm{f}}\left\{\left(\frac{\pi k_{33}}{Wd}\frac{U_\mathrm{f}}{U_\mathrm{c}}\right)^2\left[\left(\frac{U_\mathrm{c}(e_{11}+e_{33})}{\pi k_{33}}\right)^2+1\right]-1\right\}. \tag{3}$$

The threshold U_f is smaller than U_c' given by equation (2) and tends to U_c' when $e_{11}+e_{33}\rightarrow 0$. In contrast to the pure dielectric case, the deformations of the homeotropic layer may occur also when $\Delta\varepsilon>0$, but only if the relationship

$$\frac{(e_{11}+e_{33})^2}{k_{33}}>\varepsilon_0\Delta\varepsilon \tag{4}$$

is satisfied. The corresponding threshold voltage can be calculated from the equation

$$\cot\left(\pi\frac{U_\mathrm{f}}{U_\mathrm{c}}\right)=\frac{Wd}{2\pi k_{33}}\frac{U_\mathrm{c}}{U_\mathrm{f}}\left\{\left(\frac{\pi k_{33}}{Wd}\frac{U_\mathrm{f}}{U_\mathrm{c}}\right)^2\left[\left(\frac{U_\mathrm{c}(e_{11}+e_{33})}{\pi k_{33}}\right)^2-1\right]-1\right\}. \tag{5}$$

The equations (1)–(5) were derived for the case of an insulating material, ignoring the ionic space charge. However ions are unavoidable in liquid crystals and may influence the behaviour of the layer. The deformations can also be affected by the surface polarization or selective adsorption of ions [7–9]. These phenomena give rise to a surface electric field. The electrostatic interactions between this field and the nematic may influence the boundary conditions which are essential for the deformation.

In this paper, we have reanalysed numerically the electric field-induced deformations of a conductive nematic possessing flexoelectric properties. The role of the surface polarization was also considered. Our main aims were: (i) to find the director configurations in the layers deformed by various voltages, and (ii) to determine the influence of the anchoring strength, ion concentration and flexoelectric coefficients on these configurations. We chose the homeotropic layer as an example. The results of our calculations show that the threshold voltage can be significantly lowered by the space charge. Under suitable conditions, the threshold voltage can be one order of magnitude smaller than the theoretical value, equation (3), predicted for the ideal insulating nematic. The surface polarization influences the director orientation and the potential distribution but has only a minor effect on the threshold voltages.

In the next section, the parameters of the system under consideration and the basic equations are given. In §3, the results of calculations are presented; §4 is devoted to a short discussion.

2. Method

2.1. *Geometry and parameters*

A nematic liquid crystal layer of thickness $d=20\,\mu\mathrm{m}$, confined between two infinite plates parallel to the xy plane of the Cartesian co-ordinate system and positioned at $z=\pm d/2$, was considered. Homeotropic alignment was assumed. The material parameters used in calculations were typical for nematic liquid crystals. The anchoring strength W was identical on both surfaces and was varied from 10^{-5} to $10^{-2}\,\mathrm{J\,m^{-2}}$. Both signs of the dielectric anisotropy were taken into account. The elastic constants $k_{11}=6.2\times10^{-12}\,\mathrm{N}$ and $k_{33}=8.6\times10^{-12}\,\mathrm{N}$ were adopted. The sum of the flexoelectric coefficients $e=e_{11}+e_{33}$ was changed between 0 and $-40\times10^{-12}\,\mathrm{C\,m^{-1}}$ which covers most of the existing data [3]. (The individual values of e_{11} and e_{33} are not essential in the considered geometry.) Perfectly blocking electrodes were assumed. The voltage U was applied between them; the lower electrode ($z=-d/2$) was earthed. The average ion concentration N_0 ranged from 10^{18} to $10^{20}\,\mathrm{m^{-3}}$. The director $\mathbf{n}$ was assumed to be confined in the xz plane; its orientation was described by the angle $\theta(z)$ between $\mathbf{n}$ and the z axis.

The surface polarization $\mathbf{P}_s$ was assumed to be induced by the *ordo*-electric mechanism [5, 9, 10] and considered in the manner applied in our previous paper [11]. It was directed along the z axis. Its value decreased exponentially with distance from the boundaries according to the formula

$$P_s(\zeta) = (1/2)P\left[3\cos^2\theta(\zeta) - 1\right] \{\exp[-(\zeta+0.5)/\lambda] + \exp[(\zeta-0.5)/\lambda]\} \quad (6)$$

where $\zeta = z/d$, $\lambda = L/d$ and L is the characteristic length. (The value $L = 50\,\text{nm}$ was chosen arbitrarily. Its exact value is not essential for the qualitative character of the phenomena studied.) We used the value of P obtained from the relationship $m = PL$, where m is the effective dipole moment counted per unit area of the layer, identical for both surfaces. Its magnitude, as well as the sense of the dipole moment vector $\mathbf{m}$, was based on the results obtained by Blinov *et al.* [12] for the homeotropically aligning surface: $\mathbf{m}(0,0,\pm m)$ for $\zeta = \pm 1/2$, where $m = 4\times10^{-12}\,\text{C m}^{-1}$.

2.2. *Basic equations*

The problem is considered to be one-dimensional. The functions $\theta(\zeta)$ and $V(\zeta)$ which describe the director orientation and the potential distribution within the layer are determined by the torque equation:

$$\frac{1}{2}(k_b - 1)\sin 2\theta\left(\frac{d\theta}{d\zeta}\right)^2 - \left(\sin^2\theta + k_b\cos^2\theta\right)\frac{d^2\theta}{d\zeta^2} + \frac{1}{2}\frac{\varepsilon_0\Delta\varepsilon}{k_{11}}\sin 2\theta\left(\frac{dV}{d\zeta}\right)^2 + \frac{1}{2}\left(\frac{e_{11}+e_{33}}{k_{11}}\right)\sin 2\theta\left(\frac{d^2V}{d\zeta^2}\right) + \frac{3}{2}\frac{m}{k_{11}\lambda}\sin 2\theta\exp[-1/(2\lambda)][\exp(-\zeta/\lambda) - \exp(\zeta/\lambda)]\frac{dV}{d\zeta} = 0 \quad (7)$$

and the electrostatic equation:

$$\rho(\zeta)d^2 + \varepsilon_0\left(\varepsilon_\perp + \Delta\varepsilon\cos^2\theta\right)\frac{\partial^2 V}{\partial\zeta^2} - \varepsilon_0\Delta\varepsilon\sin 2\theta\frac{\partial V}{\partial\zeta}\frac{\partial\theta}{\partial\zeta} + (e_{11}+e_{33})\cos 2\theta\left(\frac{\partial\theta}{\partial\zeta}\right)^2 + \frac{1}{2}(e_{11}+e_{33})\sin 2\theta\frac{\partial^2\theta}{\partial\zeta^2} - \frac{3}{2}\frac{m}{\lambda}\exp[-1/(2\lambda)]\left\{\sin 2\theta\frac{\partial\theta}{\partial\zeta}[\exp(-\zeta/\lambda) - \exp(\zeta/\lambda)] + \frac{1}{\lambda}\left(\cos^2\theta - \frac{1}{3}\right)[\exp(-\zeta/\lambda) + \exp(\zeta/\lambda)]\right\} = 0 \quad (8)$$

where $k_b = k_{33}/k_{11}$. The space charge density $\rho(\zeta)$ results from the assumption that the ions in the nematic liquid obey Boltzmann statistics:

$$\rho(\zeta) = q[N_+(\zeta) - N_-(\zeta)] = N_0 q\left[\frac{\exp[-V(\zeta)q/k_BT]}{\int_{-1/2}^{1/2}\exp[-V(\zeta)q/k_BT]d\zeta} - \frac{\exp[V(\zeta)q/k_BT]}{\int_{-1/2}^{1/2}\exp[V(\zeta)q/k_BT]d\zeta}\right] \quad (9)$$

where $N_+(\zeta)$ and $N_-(\zeta)$ denote the concentrations of ions of both signs, q is the absolute value of the ionic charge, k_B is the Boltzmann constant and T is the absolute temperature ($T = 300\,\text{K}$). The functions $N_\pm(\zeta)$ depend on the potential distribution, which, on the other hand, is influenced by the ion distribution. A similar approach was applied in [11] and [13]. The boundary conditions for $\theta(\zeta)$ are determined by the equations

$$\pm\left\{\frac{1}{2}\left(\frac{e_{11}+e_{33}}{k_{11}}\right)\sin 2\theta(\pm 1/2)\left.\frac{dV}{d\zeta}\right|_{\pm 1/2} - \left[\sin^2\theta(\pm 1/2) + k_b\cos^2\theta(\pm 1/2)\right]\left.\frac{d\theta}{d\zeta}\right|_{\pm 1/2}\right\} - \frac{1}{2}\gamma\sin 2\theta(\pm 1/2) = 0 \quad (10)$$

for $\zeta = \pm 1/2$, where $\gamma = Wd/k_{11}$. The boundary conditions for the potential are $V(-1/2) = 0$ and $V(1/2) = U$.

The set of equations (7) and (8) was solved numerically. The director configurations [described by the angle $\theta(\zeta)$] and the electric potential distributions $V(\zeta)$ were calculated for various voltages and layer parameters. The results allowed us to determine the threshold voltages U_T for the deformations. The volume space charge density distributions $\rho(\zeta)$ were also calculated from equation (9).

3. Results

3.1. *Negative dielectric anisotropy*

In the case of negative dielectric anisotropy, the deformations have both dielectric and flexoelectric origins. The dielectric properties of the model substance used in this part of our calculations were determined by $\Delta\varepsilon = -0.7$ and $\varepsilon_\perp = 5.4$. Figure 1 gives a comparison of the representative director distributions for the flexoelectric and non-flexoelectric nematic, significantly deformed under weak and strong boundary anchoring conditions, in the presence and in the absence of the ions (curves 1–8). The deformation of

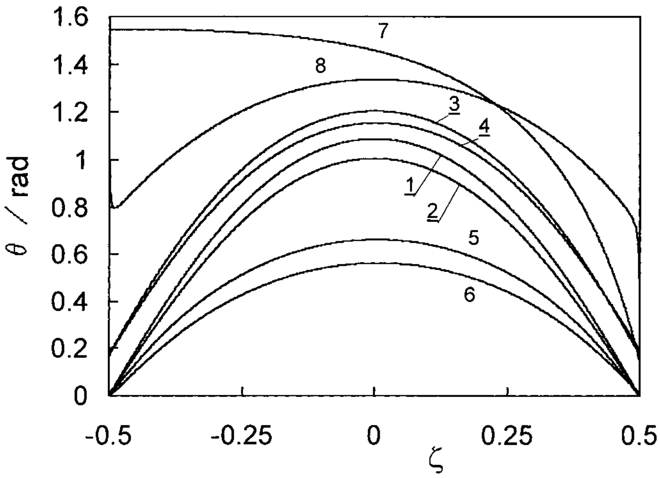

Figure 1. Director orientation angle θ as a function of the reduced coordinate ζ in the layer; $U=5\,\mathrm{V}$; $\Delta\varepsilon<0$; the parameters for curves 1–8 are as follows. 1: $e=0$, $N_0=0$, $W=10^{-2}\,\mathrm{J\,m^{-2}}$; 2: $e=0$, $N_0=10^{20}\,\mathrm{m^{-3}}$, $W=10^{-2}\,\mathrm{J\,m^{-2}}$; 3: $e=0$, $N_0=0$, $W=10^{-5}\,\mathrm{J\,m^{-2}}$; 4: $e=0$, $N_0=10^{20}\,\mathrm{m^{-3}}$, $W=10^{-5}\,\mathrm{J\,m^{-2}}$; 5: $e=-40\times10^{-12}\,\mathrm{C\,m^{-1}}$, $N_0=0$, $W=10^{-2}\,\mathrm{J\,m^{-2}}$; 6: $e=-40\times10^{-12}\,\mathrm{C\,m^{-1}}$, $N_0=10^{20}\,\mathrm{m^{-3}}$, $W=10^{-2}\,\mathrm{J\,m^{-2}}$; 7: $e=-40\times10^{-12}\,\mathrm{C\,m^{-1}}$, $N_0=0$, $W=10^{-5}\,\mathrm{J\,m^{-2}}$; 8: $e=-40\times10^{-12}\,\mathrm{C\,m^{-1}}$, $N_0=10^{20}\,\mathrm{m^{-3}}$, $W=10^{-5}\,\mathrm{J\,m^{-2}}$.

the strongly anchored nematics (curves 1, 2, 5 and 6) and of the weakly anchored non-flexoelectric nematics (curves 3 and 4) are symmetrical, *i.e.* described by even $\theta(\zeta)$ functions. In the case of strong anchoring, the flexoelectric properties manifest themselves by weakening of the deformation (cf. Curves 5 *vs.* 1 and 6 *vs.* 2) while the director distribution remains symmetrical. Well developed deformations of a flexoelectric nature arise under weak anchoring conditions. They are distinguishable by the asymmetry of the director distribution (curves 7 and 8). In the case of a weakly anchored non-flexoelectric material, the director at the surfaces deviates from the homeotropic orientation (curves 3 and 4). The behaviour of the insulating nematic illustrated by curves 1, 3, 5 and 7 is well known. The presence of the ionic space charge diminishes the director deviation from the initial alignment (cf. curves 4 *vs.* 3, 2 *vs.* 1 and 6 *vs.* 5). The effect of ions is always present but is particularly pronounced in a weakly anchored flexoelectric material for which the director orientation in the vicinity of the boundaries is changed significantly (curve 8). Therefore the results concerning the deformations occurring in a weakly anchored flexoelectric nematic with a significant ion concentration N_0 are the most interesting.

The most essential features of these deformations are as follows:

(i) The threshold voltage value can be high or low depending on the parameters of the layer. The high values are equal to several volts, the low amount to a few tenths of a volt.

(ii) The director distributions vary qualitatively when the voltage is changed. The changes are particularly marked in the case of the low threshold.

Figures 2, 3 and 4 show the dependences of the threshold voltage U_T on N_0, W and $|e_{11}+e_{33}|$, respectively. For strong anchoring or low ion concentrations or small absolute values of the flexoelectric coefficients, the threshold voltage amounts to several volts and is approximately constant over wide range of these parameters. Its value is comparable to the theoretical results expressed by equation (3). The threshold decreases to a few tenths of a volt when simultaneously the anchoring is weak, the ion concentration

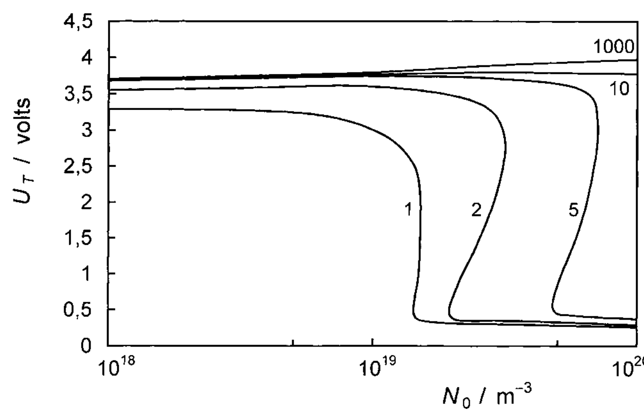

Figure 2. The threshold voltage U_T as a function of the ion concentration N_0; $e=-40\times10^{-12}\,\mathrm{C\,m^{-1}}$, $\Delta\varepsilon<0$; the anchoring energies W (in $10^{-5}\,\mathrm{J\,m^{-2}}$) are indicated at each curve.

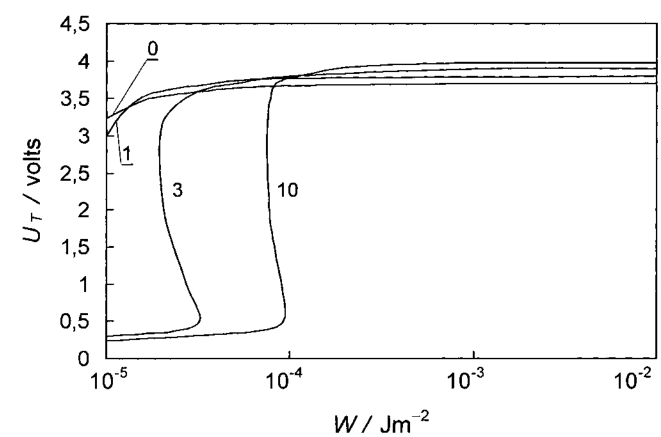

Figure 3. The threshold voltage U_T as a function of the anchoring energy W; $e=-40\times10^{-12}\,\mathrm{C\,m^{-1}}$, $\Delta\varepsilon<0$; the ion concentrations N_0 (in $10^{19}\,\mathrm{m^{-3}}$) are indicated at each curve.

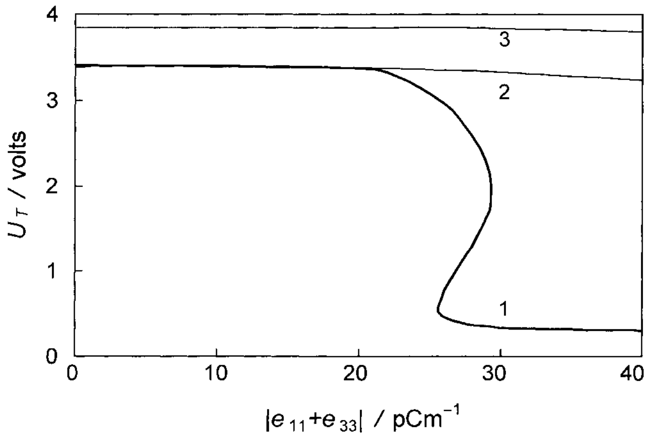

Figure 4. The threshold voltage U_T as a function of the sum of flexoelectric coefficients $|e_{11}+e_{33}|$; $\Delta\varepsilon<0$. 1: $W=10^{-5}\,\mathrm{J\,m^{-2}}$, $N_0=3\times10^{19}\,\mathrm{m^{-3}}$; 2: $W=10^{-5}\,\mathrm{J\,m^{-2}}$, no ions; 3: $W=10^{-4}\,\mathrm{J\,m^{-2}}$, $N_0=3\times10^{19}\,\mathrm{m^{-3}}$.

is high and the flexoelectric coefficients have large magnitude. There exist also intermediate values of these parameters for which the layer is distorted in two ranges of voltage and remains undisturbed between them. Two thresholds for deformations exist in such layers.

The director profiles corresponding to the deformations initiated at low threshold are shown in figure 5 for several representative voltages. The qualitative differences between them are evident. Various types of profile occur in various voltage ranges, the transitions between subsequent types having threshold character. The deformations arise rapidly above the threshold U_T. The director deviates from its initial orientation by an angle increasing with z, with the exception of thin layers of thickness 0.5 μm adjacent to the boundary plates. At higher voltages, the greatest deviation takes place in the middle part of the layer; simultaneously, the subsurface deformations change their form.

In the case of a high value of the threshold resulting from low ion concentration, the director distribution is similar to that illustrated by curve 7 in figure 1. When the high threshold is due to strong surface anchoring, the director profiles are nearly symmetric. The slight deviation from exact symmetry is due to the flexoelectric properties that induce some distortions near the boundaries. As a result, the deformations are qualitatively similar to that given by curve 8.

3.2. *Positive dielectric anisotropy*

In the case of $\Delta\varepsilon>0$, the homeotropic layer is dielectrically stable. The torque due to the flexoelectric properties is the only cause of the deformations. Equation (4) yields a condition for this deformation. In order to verify this relationship in the presence of ionic space charge, we studied the behaviour of the nematic characterized by various $\Delta\varepsilon$ values. The crucial role of the space charge was confirmed. Figure 6 shows the threshold voltage plotted as a function of the dielectric anisotropy for several values of ion concentration. As previously, two regimes of the threshold voltage can be distinguished. They are connected with two types of behaviour.

(i) If $\Delta\varepsilon$ is sufficiently high, or if N_0 is sufficiently low, the threshold voltage U_T increases with $\Delta\varepsilon$, which resembles the dependence predicted by equation (5) for insulating materials. The deformations of the director field are restricted to the

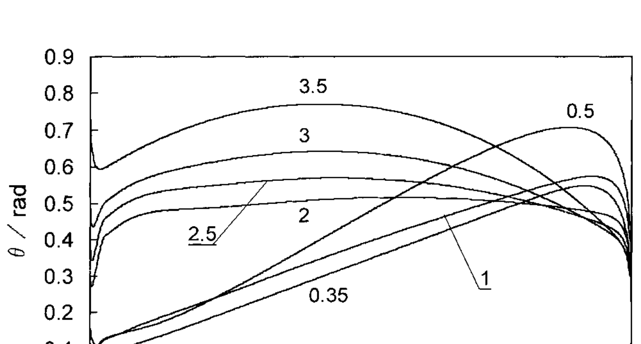

Figure 5. Director orientation angle θ as a function of the reduced coordinate ζ; $W=10^{-5}\,\mathrm{J\,m^{-2}}$, $N_0=3\times10^{19}\,\mathrm{m^{-3}}$, $e=-40\times10^{-12}\,\mathrm{C\,m^{-1}}$, $\Delta\varepsilon<0$; (the low threshold case, $U_T=0.28\,\mathrm{V}$); the applied voltage U (in volts) is indicated at each curve.

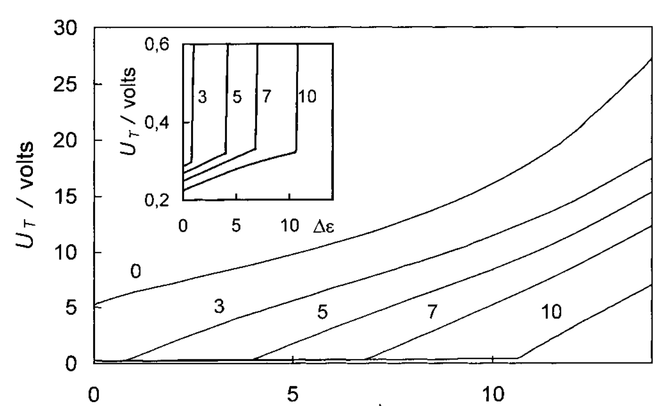

Figure 6. The threshold voltage U_T as a function of the positive dielectric anisotropy $\Delta\varepsilon$; $W=10^{-5}\,\mathrm{J\,m^{-2}}$, $e=-40\times10^{-12}\,\mathrm{C\,m^{-1}}$; the ion concentration N_0 (in $10^{19}\,\mathrm{m^{-3}}$) is indicated at each curve; the inset shows the details of the $U_T(\Delta\varepsilon)$ dependences in the low threshold regime.

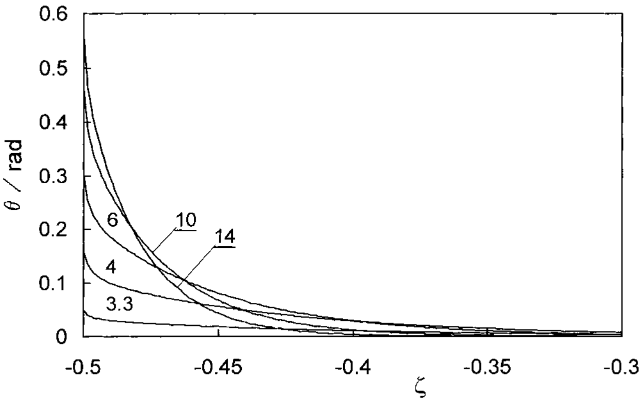

Figure 7. Director orientation angle θ as a function of the reduced coordinate ζ; positive dielectric anisotropy $\Delta\varepsilon = 12$, $W = 10^{-5}\,\mathrm{J\,m^{-2}}$, $N_0 = 10^{20}\,\mathrm{m^{-3}}$, $e = -40 \times 10^{-12}\,\mathrm{C\,m^{-1}}$; (the high threshold case, $U_T = 3.2\,\mathrm{V}$); the applied voltage U (in volts) is indicated at each curve.

thin layer adjacent to one of the boundary plates, as shown by the $\theta(\zeta)$ profiles plotted in figure 7. The thickness of this layer is of the order of 1 μm and decreases with the voltage.

(ii) In the opposite case, *i.e.* in weakly anisotropic and highly conductive materials, the deformations arise at some low threshold voltage which amounts to a few tenths of a volt and is nearly independent of $\Delta\varepsilon$ and N_0. For a typical ion concentration of $10^{20}\,\mathrm{m^{-3}}$, this behaviour is predicted for materials with $\Delta\varepsilon < 11$. The deformations are described by the $\theta(\zeta)$ functions shown in figure 8; they develop rapidly when the voltage exceeds the threshold. The strongest distortions appear in the neighbourhood of the boundaries. At low voltages the director distribution is similar to that occurring in the case of $\Delta\varepsilon < 0$. The form of the director profiles varies with the voltage; at high voltages, the deformations are similar to those taking place in the high threshold case.

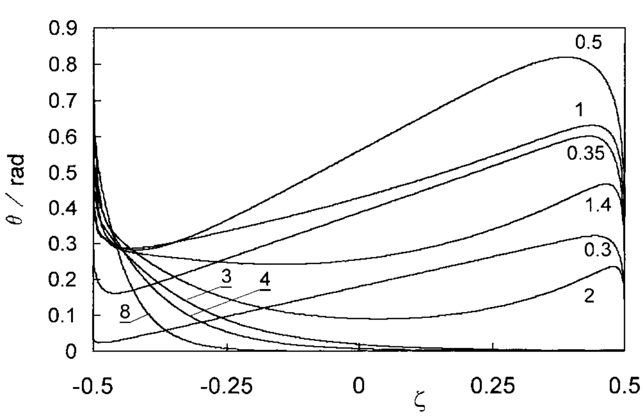

Figure 8. Director orientation angle θ as a function of the reduced coordinate ζ; positive dielectric anisotropy $\Delta\varepsilon = 5$, $W = 10^{-5}\,\mathrm{J\,m^{-2}}$, $N_0 = 10^{20}\,\mathrm{m^{-3}}$, $e = -40 \times 10^{-12}\,\mathrm{C\,m^{-1}}$; (the low threshold case, $U_T = 0.28\,\mathrm{V}$); the applied voltage U (in volts) is indicated at each curve.

The condition expressed by the inequality (4) is not valid in the presence of ions. A less restrictive condition applies, *i.e.* for a given $\Delta\varepsilon$ and k_{33}, the deformation may arise even if the sum $|e_{11} + e_{33}|$ is smaller than $(\varepsilon_0 \Delta\varepsilon / k_{33})^{\frac{1}{2}}$. However the numerically calculated threshold reaches tens of volts whereas the deformation is extremely small and limited to the vicinity of the boundary.

3.3. *Influence of the surface polarization*

The influence of the surface polarization was studied for a negative dielectric anisotropy. The surface polarization changes the director configuration in the layer, the greatest effect being found in the case of low threshold. Under suitable circumstances, the director profiles calculated for $m = 0$ and $m \neq 0$ are different, as shown in figure 9. The surface polarization diminishes the deformations in the interior of the layer and enhances the distortions near $z = d/2$. Neither the low nor the high threshold voltage is influenced significantly. Their values for $m \neq 0$ are smaller than those for $m = 0$ only by several percent.

The potential distribution is also modified by the surface polarization. For $m = 0$ the spatial dependence of the electric field strength value is given by the nearly even function $E(\zeta)$. This symmetry is disturbed by the

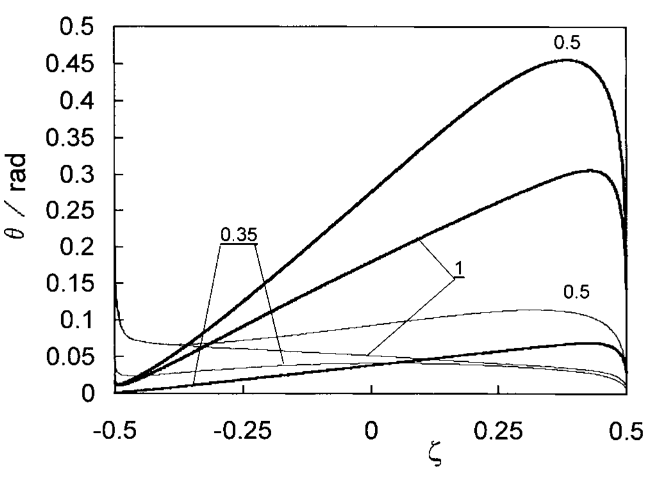

Figure 9. Comparison of the director profiles calculated for $m = 0$ (thick lines) and $m = 4 \times 10^{-12}\,\mathrm{C\,m^{-1}}$ (thin lines); $W = 2 \times 10^{-5}\,\mathrm{J\,m^{-2}}$, $N_0 = 3 \times 10^{19}\,\mathrm{m^{-3}}$, $e = -40 \times 10^{-12}\,\mathrm{C\,m^{-1}}$, $\Delta\varepsilon < 0$; (the low threshold case); the applied voltages U (in volts) are indicated at each curve.

field originating in the surface polarization, which has a strength comparable to that of the bias field but its sign at $\zeta = 1/2$ is opposite.

3.4. *Space charge distribution*

The space charge density $\rho(\zeta)$ was determined from equation (9) by use of the calculated $V(\zeta)$ functions. In general, ions of opposite signs are swept towards the electrodes. No peculiarities in their spatial distribution were found. At low voltages, positive ions are removed from the neighbourhood of the positive electrode. Their concentration in the interior of the layer is three orders of magnitude lower than the maximum concentration at the negative electrode (*e.g.* at 0.35 V). The distribution of the negative ions is analogous. At sufficiently high voltage (*e.g.* 2 V), the interior of the layer is practically free from ions. They occupy thin layers at the boundary plates.

4. Discussion

In this paper, we have considered the deformations of the flexoelectric nematic liquid crystal induced by a bias d.c. voltage. They are often referred to as the converse flexoelectric effect [3]. Our results show that under suitable circumstances, remarkable deformations arise at relatively low thresholds due to the presence of ions.

The qualitative explanation of this effect can be based on an analysis of the electric field distribution (figure 10). Under the action of an external voltage, ions of opposite sign accumulate in the vicinity of the electrodes. In consequence, the electric field in thin layers adjacent to the boundary plates is enhanced significantly. Its strength may reach remarkable values even at low voltages and depends strongly on the

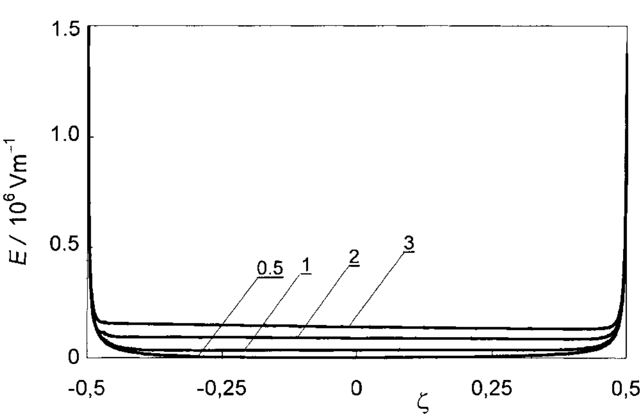

Figure 10. Electric field strength $E(\zeta)$ in the layer; $W = 10^{-5}\,\mathrm{J\,m^{-2}}$, $N_0 = 3 \times 10^{19}\,\mathrm{m^{-3}}$, $e = -40 \times 10^{-12}\,\mathrm{C\,m^{-1}}$; $\Delta\varepsilon < 0$; (the low threshold case, $U_T = 0.28\,\mathrm{V}$); the applied voltage U (in volts) is indicated at each curve.

distance from the electrodes. The surface field strength E exceeds the value U/d by nearly two orders of magnitude, for instance when $N_0 = 3 \times 10^{19}\,\mathrm{m^{-3}}$ and $U = 0.5\,\mathrm{V}$, the field strength $E(-1/2)$ amounts $1.45 \times 10^6\,\mathrm{V\,m^{-1}}$ whereas $U/d = 2.50 \times 10^4\,\mathrm{V\,m^{-1}}$. Both E and $\mathrm{d}E/\mathrm{d}z$ increase with ion concentration. They are weakly dependent on voltage and almost independent of anchoring energy.

The dielectric and flexoelectric torques exerted on the director by this inhomogeneous field [expressed by the third and fourth components of equation (7)] are much greater than the torques acting in the bulk of the layer where the field is nearly constant or may even be totally cancelled at low voltages. In particular, the flexoelectric torque may be strong enough to induce subsurface distortions, thus changing dramatically the circumstances which determine the director orientation in the bulk. If the anchoring is sufficiently weak and the flexoelectric properties are sufficiently strong and the positive dielectric anisotropy is not too high, the deformation can be initiated at a threshold voltage as low as a few tenths of a volt. The resulting director distribution may be quite different from that predicted for the insulating nematic. The variety of the director profiles shown in figures 5, 8 and 9 illustrates the delicate interplay of all the kinds of torques involved in the problem. (An analogous effect can be recognized in the results of [13] where the director profiles for the hybrid aligned nematic layer are presented. For certain voltages, they reveal strong distortions at the surfaces and do not resemble the plots theoretically predicted for the insulating hybrid aligned layer.)

A comparison of the two low threshold behaviours presented in figures 5 and 8 indicates the similarity of the profiles obtained for $\Delta\varepsilon < 0$ and $\Delta\varepsilon > 0$ at voltages lower than *c.* 1 V. This suggests that the deformations are initiated by the same mechanism in each case. As the dielectric anisotropies have different signs, the flexoelectricity is expected to be the common origin of the deformations. At higher voltages, the deformations evolve according to the sign of dielectric anisotropy; they are enhanced if $\Delta\varepsilon < 0$ and suppressed in the opposite case. In both situations, the director profiles in the interior of the layer resemble the distributions typical for dielectrically deformed non-flexoelectric nematics. Nevertheless, the consequences of the flexoelectric properties are still visible, especially in the vicinity of the surfaces.

Our calculations yield examples of some other effects caused by the ions. Under rigid anchoring conditions, the presence of the ionic space charge is manifested by a slight decrease of the director deviation from its initial alignment (curves 5 and 6 in figure 1) which is probably due to the decrease of the effective electric field strength in the bulk. Strong anchoring excludes any boundary effects and no evidence of the flexoelectric properties can be seen. Deformations of flexoelectric nature can arise if the anchoring is weak. The corresponding director profiles are not symmetrical. A comparison of curves 7 and 8 in figure 1 shows that the asymmetry in the interior of the layer disappears at high ion concentration. In consequence, the bulk director profile becomes similar to the non-flexoelectric case with sufficiently weak anchoring. Flexoelectric properties are revealed only by distortions in the vicinity of the boundaries.

The surface polarization yields additional contributions to the electric field. In our case, this additional field has different senses on the two boundaries and its strength is comparable to that of the bias field; it therefore changes the director distribution and its evolution with increasing voltage.

In earlier theoretical works [7–9], the surface electric field was found to be the reason for the significant change in behaviour of the layer. The fields due to the adsorption of ions and to surface polarization were taken into account. It was stated that the surface field can affect the bulk distribution of the director by distorting the director orientation near the surface. The deformation occurs above a suitable threshold value of the surface field [8]. The contribution of the surface field can be interpreted as a change of the effective anchoring strength [9]; it also changes the effective flexoelectric coefficients [7]. These results strongly support our qualitative explanation concerning the role of the surface field arising from the separation of ions in the external field.

The results of numerical computations presented in this paper require experimental verification. The homeotropic nematic layer subjected to a d.c. electric field belongs to well known liquid crystalline systems; however, as far as we know, no experimental evidence of the 'low threshold' deformations in this geometry has been reported. It seems plausible that the usual anchoring energies are too high and exclude this phenomenon. Probably the boundary surfaces should be specially prepared to allow the distortions at low voltages. Nevertheless, effects resembling our results are reported in [14] where deformations of the planar nematic layers in a perpendicular d.c. electric field are described. The deformations were observed at voltages as low as 0.05 V. The decrease in ion concentration led to the decay of the deformations.

Arguments similar to those presented here were used in [15] to explain some high field electro-optic effects observed in $\Delta\varepsilon > 0$ nematic samples. Ions that are swept towards the electrode produce a strongly non-uniform electric field, which couples with the flexoelectric polarization and gives rise to deformation.

Summarizing, our results show that the space charges redistributed by the external voltage may change significantly the effective boundary conditions. They should be taken into account when the behaviour of a weakly anchored flexoelectric nematic subjected to a d.c. electric field is studied.

References

[1] Blinov, L. M., and Chigrinov, V. G., 1993, *Electro-optic Effects in Liquid Crystal Materials* (New York: Springer Verlag).

[2] Rapini, A., and Papoular, M., 1969, *J. Phys. (Paris), Colloq.*, **30,** C4.

[3] Petrov, A. G., 2001, *Physical Properties of Liquid Crystals: Nematics*, edited by D. A. Dunmur, A. Fukuda, and G. R. Luckhurst (London: INSPEC), pp. 251–264.

[4] Meyer, R. B., 1969, *Phys. Rev. Lett.*, **22,** 918.

[5] Prost, J., and Marcerou, J. P., 1977, *J. Phys. (Paris)*, **38,** 315.

[6] Derzhanski, A., Petrov, A. G., and Mitov, M. D., 1978, *J. Phys. (Paris)*, **39,** 273.

[7] Barbero, G., and Durand, G., 1987, *Phys. Rev. A*, **35,** 1294.

[8] Barbero, G., Evangelista, L. R., and Madhusudana, N. V., 1998, *Eur. Phys. J. B*, **1,** 327.

[9] Zakharov, A. V., and Dong, R. Y., 2001, *Phys. Rev. E*, **64,** 042701.

[10] Barbero, G., Dozov, I., Palierne, J. F., and Durand, G., 1986, *Phys. Rev. Lett.*, **56,** 2056.

[11] Derfel, G., and Felczak, M., 2002, *Liq. Cryst.*, **29,** 889.

[12] Blinov, L. M., Barnik, M. I., Ohoka, H., Ozaki, M., Shtykov, N. M., and Yoshino, K., 2001, *Eur. Phys. J. E*, **4,** 183.

[13] Ponti, S., Ziherl, P., Ferrero, C., and Žumer, S., 1999, *Liq. Cryst.*, **26,** 1171.

[14] Derzhanski, A. I., Petrov, A. G., Khinov, Chr. P., and Markovski, B. L., 1974, *Bulg. J. Phys.*, **1,** 165.

[15] Basappa, G., and Madhusudana, N. V., 2000, *Proc. SPIE*, **4147,** 116.